Hindawi Publishing Corporation
Mathematical Problems in Engineering
Volume 2014, Article ID 985064, 6 pages
http://dx.doi.org/10.1155/2014/985064

Research Article

Fabrication of Compact Microstrip Line-Based Balun-Bandpass Filter with High Common-Mode Suppression

Chia-Mao Chen,[1] Shoou-Jinn Chang,[2] Yen-Liang Pan,[3] Cheng-Yi Chen,[4] and Cheng-Fu Yang[5]

[1] *Institute of Microelectronics and Department of Electrical Engineering, National Cheng Kung University, Tainan 701, Taiwan*
[2] *Institute of Microelectronics and Department of Electrical Engineering, Center for Micro/Nano Science and Technology, Advanced Optoelectronic Technology Center, National Cheng Kung University, Tainan 701, Taiwan*
[3] *Department of Avionic Engineering, Air Force Academy, Kaohsiung 820, Taiwan*
[4] *Department of Electrical Engineering, Cheng Shiu University, Kaohsiung 833, Taiwan*
[5] *Department of Chemical and Materials Engineering, National University of Kaohsiung, Kaohsiung 811, Taiwan*

Correspondence should be addressed to Cheng-Fu Yang; cfyang@nuk.edu.tw

Received 15 August 2014; Accepted 18 September 2014; Published 30 September 2014

Academic Editor: Teen-Hang Meen

A new type of balun-bandpass filter was proposed based on the traditional coupled-line theory and folded open-loop ring resonators (OLRRs) configuration. For that, a new device with both filter-type and balun-type characteristics was investigated and fabricated. Both magnetic and electric coupling structures were implemented to provide high performance balun-bandpass responses. The fabricated balun-bandpass filters had a wide bandwidth more than 200 MHz and a low insertion loss less than 2.51 dB at a center frequency of 2.6 GHz. The differences between the two outputs were below 0.4 dB in magnitude and within $180 \pm 7^{\circ}$ in phase. Also, the balun-bandpass filter presented an excellent common-mode rejection ratio over 25 dB in the passband. An advanced design methodology had been adopted based on EM simulation for making these designed parameters of OLRRs, microstrip lines, and open stubs. The measured frequency responses agreed well with simulated ones.

1. Introduction

Band-pass-filters (BPF) and baluns are critical components in the RF channels because most of the RF-front end modules require both the circuits. Integration of two functional blocks in a single circuit, which is the most intuitive way, can reduce the cost as well as the size of the designed circuit. A balun is an electrical device which can convert between a balanced signal (two signals working against each other where ground is irrelevant) and an unbalanced signal (a single signal working against ground or pseudoground). In this study, a balanced balun filter is investigated to combine a balun and a filter which provide balanced to unbalanced signal transformation and frequency discrimination. Besides having band-pass function, balanced filters are able to produce the desired differential-mode frequency response and reduce the common-mode signal at the same time. For that, balanced filters have become more and more important in the modern communication systems. Some balun BPFs are evolved from the classic quarter- and half-wavelength resonators with folding topology [1, 2]. To cater for multiband wireless systems, plenty of researches focus on the balun BPFs with multiband [3–5]. In [6], single dual-mode resonators are employed to construct a compact balun BPF.

In this paper, a generalized methodology to design a novel and simple single passband balun BPF was investigated. The low-loss balun BPF used folded open-loop ring resonators (OLRRs) with equal physical dimensions to couple two microstrip lines, as Figure 1 shows. A couple of folded OLRRs, which had a perimeter of about a half wavelength of the designed resonant frequency, were placed between two microstrip lines. The maximum electric field density was designed at around the open ends of the folded OLRRs and the maximum magnetic field density was designed at around the center valley of the folded OLRRs. The resonant frequencies could be adjusted via the length of the OLRRs

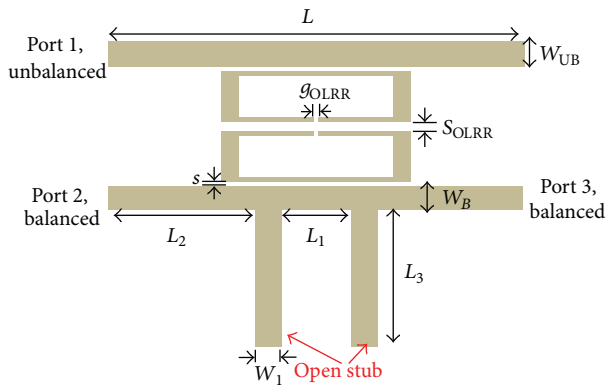

Figure 1: Proposed balun-bandpass filter (BPF) based on OLRRs.

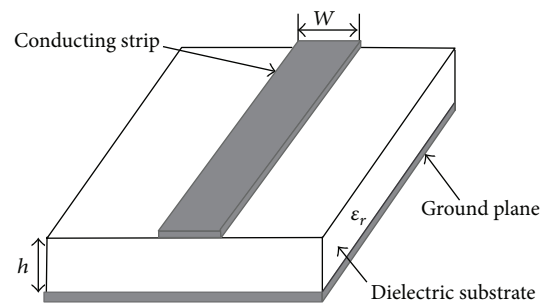

Figure 2: Microstrip transmission line structure.

to provide a high-performance passband response. The proposed balun BPF had the advantages of low insertion loss, wide tunable range of passband, large transmission zero, and simple structure. By tuning the sizes of open stubs and the length of microstrip lines, the balanced impedance of the balun BPF could also be tuned. Finally, we fabricated a high-performance balun BPF on FR4 substrates to demonstrate the proposed structure.

2. Design Methodology

Microstrip line is one of the most popular types of planar transmission lines; primarily, it can be fabricated by photolithographic process and it can easily be integrated with other passive and active microwave devices. The geometry of a microstrip line is shown in Figure 2; a conductor of width W is printed on a thin and grounded dielectric substrate of thickness d and relative permittivity ε_r. When the dimensions of a microstrip line are given, the effective dielectric constant ε_e and characteristic impedance Z_0 can be calculated from the designed formulas, which are curve-fit approximations to rigorously quasistatic solution [7]:

$$\varepsilon_e = \frac{\varepsilon_r + 1}{2} + \frac{\varepsilon_r - 1}{2} \frac{1}{\sqrt{1 + 12\,(d/W)}}, \tag{1}$$

$$Z_0 = \begin{cases} \dfrac{60}{\sqrt{\varepsilon_e}} \ln\left(\dfrac{8d}{W} + \dfrac{W}{4d}\right) & \text{for } \dfrac{W}{d} \le 1 \\ 120\pi \left(\sqrt{\varepsilon_e}\left[\dfrac{W}{d} + 1.393 + 0.667 \times \ln\left(\dfrac{W}{d} + 1.444\right)\right]\right)^{-1} & \text{for } \dfrac{W}{d} \ge 1. \end{cases} \tag{2}$$

To obtain the maximum magnetic coupling, the center valley of the OLRRs must be placed at the proper location along the microstrip line where the maximum magnetic field intensity is generated. The location can be determined by studying the wave motions on a microstrip line. For the transverse electromagnetic (TEM) field structure, both the electric and the magnetic field vectors lie in the transverse plane, which is perpendicular to the uniform propagation axis. Under the assumptions of the TEM mode of propagation and a lossless line, the fields $\vec{E}$ and $\vec{H}$ are uniquely related to voltage and current, respectively. Based on transmission line theory, the magnitudes of voltage and current on the microstrip lines can be expressed in terms of the incident wave and the reflection coefficient:

$$|V(z)| = \left|V_0^+\right| \left|1 + |\Gamma| e^{j(\theta - 2\beta l)}\right|, \tag{3}$$

$$|I(z)| = \frac{\left|V_0^+\right|}{Z_0} \left|1 - |\Gamma| e^{j(\theta - 2\beta l)}\right|, \tag{4}$$

where $l = -z$ is measured away from the load at $z = 0$ and θ is the phase of the reflection coefficient. When $\theta - 2\beta l$ has a magnitude of zero or an integer multiple of 2π radian, voltage in (3) is at its maximum magnitude and current in (4) is at its minimum magnitude, respectively. For the case of an open-circuited line, (3) and (4), respectively, become

$$\begin{aligned} |V(z)| &= \left|V_0^+\right| \left|1 + e^{j(\theta - 2\beta l)}\right|, \\ |I(z)| &= \frac{\left|V_0^+\right|}{Z_0} \left|1 - e^{j(\theta - 2\beta l)}\right|. \end{aligned} \tag{5}$$

At a distance of a quarter wavelength from the receiving end, the voltage becomes zero while the current is at its maximum. If the length of microstrip line has a value of half wavelength, the current distribution near the center of the transmission line is at its maximum. High magnetic coupling results from a high conduction current. Once the point of $I_{\max}$ is found, the point of $H_{\max}$ can be easily determined.

At a distance $l = -z$ from the load, the input impedance seen looking toward the load is

$$Z_{\text{in}} = Z_0 \frac{Z_L + jZ_0 \tan \beta l}{Z_0 + jZ_L \tan \beta l}, \tag{6}$$

where Z_0 is characteristic impedance and Z_L is load impedance. Consider first that the transmission line circuit is short circuit; it means $Z_L = 0$. From (6), the input impedance is

$$Z_{\text{in}} = jZ_0 \tan \beta l \tag{7}$$

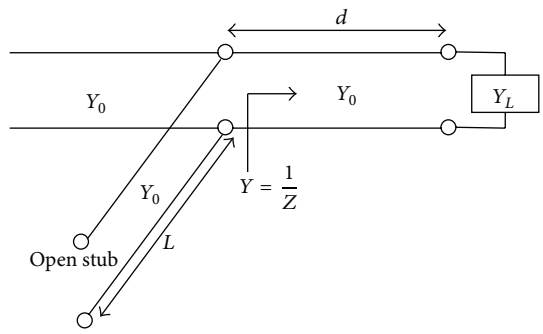

Figure 3: Single-stub tuning circuits.

which is seen to be purely imaginary for any length, l, and to take on all values between $-j\infty$ and $+j\infty$. For example, when $l = 0$, we have $Z_{\text{in}} = 0$, but for $l = \lambda/4$, we have $Z_{\text{in}} = \infty$ (open circuit). Equation (7) also shows that the impedance is periodic in l, repeating for an integer multiple of $\lambda/2$. Next consider that the transmission line circuit is open circuit, $Z_L = \infty$. From (6), the input impedance is

$$Z_{\text{in}} = -jZ_0 \cot \beta l \tag{8}$$

which is also purely imaginary for any length, l.

In this paper, we used a matching technique, which employed a single open-circuited length of transmission line (a "stub"), to connect in parallel with the transmission feed line at a certain distance from the load, as shown in Figure 3. Such a tuning circuit is convenient from a microwave fabrication aspect, since lumped elements are not required. In single-stub tuning, the two adjustable parameters are the distance, d, from the load to the stub position and the value of susceptance by the shunt stub. The basic idea is to select d so that the admittance, Y, seen looking into the line at distance d from the load is of the form $Y_0 + jB$. Then the stub susceptance is chosen as $-jB$, resulting in a matched condition.

Figure 4(a) shows the structure of the proposed stub-loaded resonator. Under differential-mode operation, a virtual-short condition appears along the symmetric line, leading to the approximated differential-mode bisection in Figure 4(b). The resulted differential-mode input impedance can be written as

$$Z_{\text{in},B} = Z_{01} \frac{Z_1 + jZ_{01} \tan \beta L_2}{Z_{01} + jZ_1 \tan \beta L_2}, \tag{9}$$

where

$$\begin{aligned} Z_1 &= \left\{ \left[jZ_{01} \tan \beta \left(\frac{L_2}{2} \right) \right] // \left(-jZ_{02} \cot \beta L_3 \right) \right\} \\ &= \left\{ \left[jZ_{01} \tan \beta \left(\frac{L_2}{2} \right) \right]^{-1} + \left(-jZ_{02} \cot \beta L_3 \right)^{-1} \right\}^{-1}. \end{aligned} \tag{10}$$

To demonstrate the proposed structure is available, the balun BPF is designed using OLRRs to couple microstrip transmission lines. To excite the passbands, a pair of guided half-wavelength OLRRs should be located between two microstrip lines. The OLRRs provide a path coupled signal energy from one microstrip line to another one at around resonance frequency. When the signal is at the resonance frequency, most of the energy is reflected back and the standing waves are said to exist on the lines. After that, the designed balun BPFs were simulated using the HFSS simulator with loss factors (conductor loss and dielectric loss), included in the simulated response to find the optimal parameters.

Besides having good match in input impedance and good amplitude and phase balances between the two output ports, the match in output balanced impedance will make balun BPFs having more attraction in the sense of the system integration ability. The structures of using microstrip lines and open stubs are very easy for us to tune balanced impedance, because we only need to adjust the width (W_B) of balanced-port microstrip lines and add different lengths of open stub, as the structure shown in Figure 1. To characterize the balance characteristic of the balun BPFs, the mode conversion between the unbalanced three-port network and the unbalanced-to-balanced two-port network is applied to obtain the single-ended to differential-mode and common-mode parameters; they can be obtained from the following equation [8, 9]:

$$\begin{aligned} S_{ss11} &= S_{11}, \qquad S_{ds21} = \frac{(S_{21} - S_{31})}{\sqrt{2}}, \\ S_{cs21} &= \frac{(S_{21} + S_{31})}{\sqrt{2}}, \end{aligned} \tag{11}$$

where S_{ss11} is the return loss at the unbalanced port 1, S_{ds21} is the two-port S-parameters from the unbalanced port 1 to differential-mode balanced port 2, and S_{cs21} is the two-port S-parameters from the unbalanced port 1 to common-mode balanced port 2, respectively.

3. Design of Balun-Bandpass Filters

The balun BPF using OLRRs was fabricated on an FR4 substrate with a relative permittivity of 4.4, and a thickness between the two electrodes was 1.0 mm (W_{UB}). From (2), the width of 50 Ω microstrip line was about 2 mm. The designed balun BPF was based on a pair of half-wavelength OLRRs. Electrical coupling could be obtained if the open sides of the two coupled resonators were placed near each other, and magnetic coupling could be obtained if the sides with the maximum magnetic field of two coupled resonators were placed near each other. The coupling spacing S between the microstrip lines and OLRRs was 0.2 mm and the spacing S_{OLRR} between two resonators was 0.61 mm. Once the correct position was chosen, the center frequency of the designed balun BPF could be accurately controlled to a desired frequency. In this study, the balun BPF with central frequency of 2.6 GHz was designed and investigated. The simulation result of the designed balun BPF showed good match in input impedance, good amplitude and phase balances between the two output ports, and a wide passband, respectively. Those

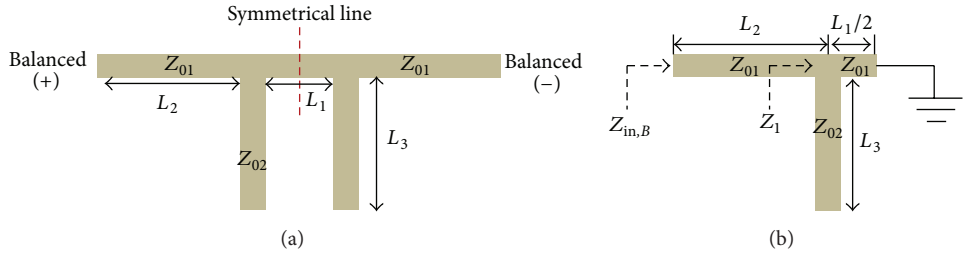

Figure 4: (a) Structure of the proposed stub-loaded resonator. (b) Differential mode equivalent bisection.

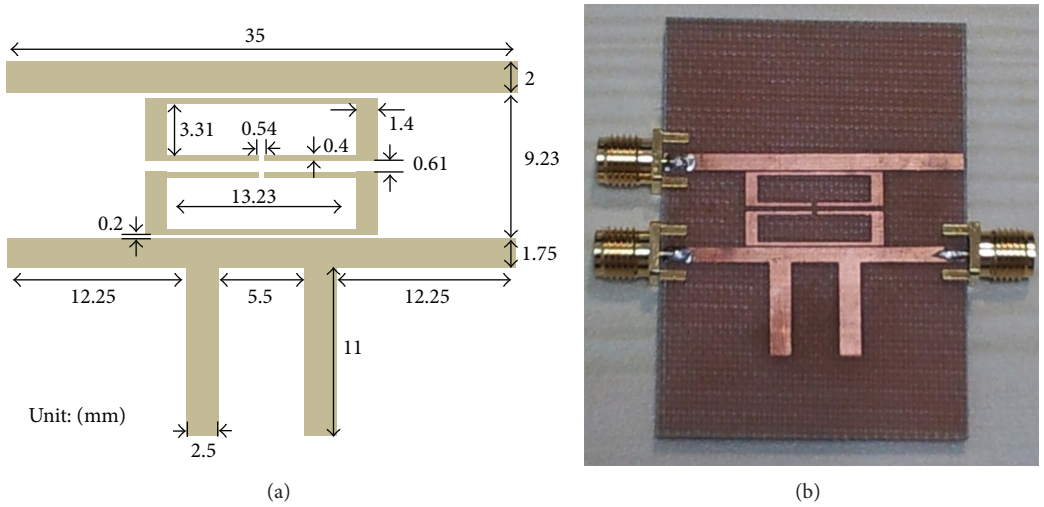

Figure 5: (a) Layout pattern and (b) photograph of the designed balun BPF with about 100 Ω balanced impedance.

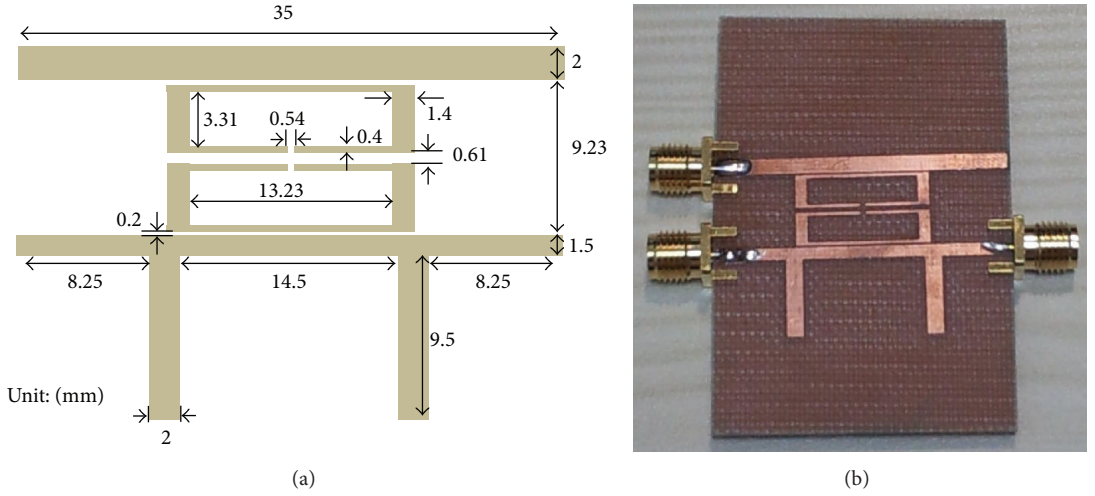

Figure 6: (a) Layout pattern and (b) photograph of the designed balun BPF with about 50 Ω balanced impedance.

simulated results prove that we only needed to find the optimum width (W_B) of balanced-port microstrip line and add open stub and then we could tune balanced impedance. The differently balanced impedances of the designed balun BPFs with open stub are shown in Table 1.

Both patterns in Figures 5 and 6 have the same designed structures. In order to design the balanced impedance that is needed, the lengths of open stub and the values of W_B in both Figures 5 and 6 were different from each other. The dimension for the proposed balun BPF with balanced impedance of 100 Ohm was 35 mm × 23.98 mm, as shown in Figure 5(a), and the photograph of the fabricated balun BPF is shown in Figure 5(b). Similarly, the dimension for the proposed balun BPF with balanced impedance of 50 Ohm

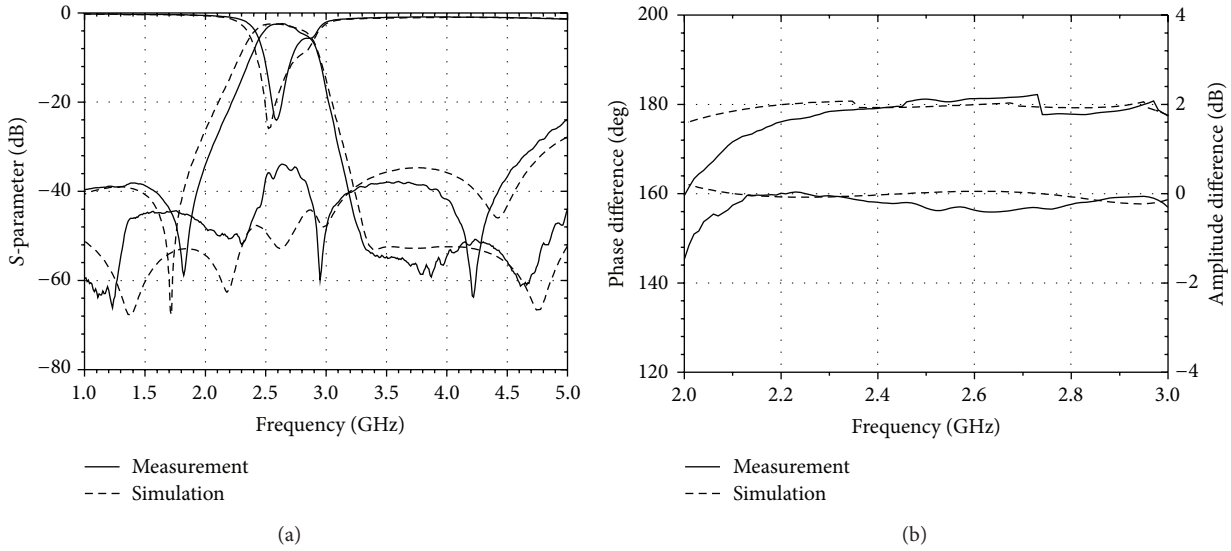

Figure 7: (a) S-parameters and (b) phase/amplitude differences of the designed balun BPF with about 100 Ω balanced impedance.

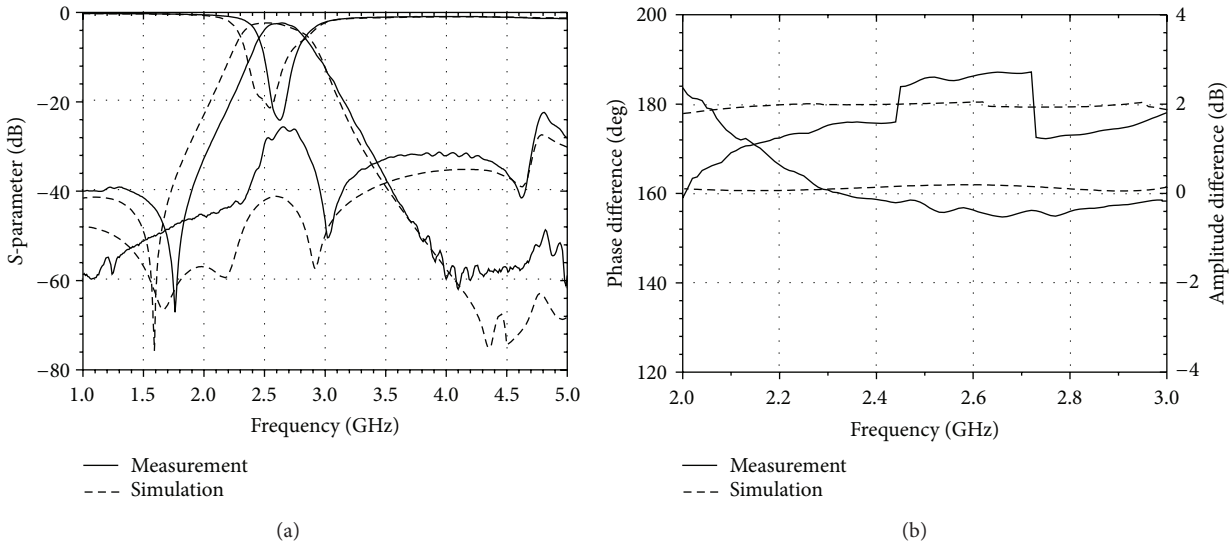

Figure 8: (a) S-parameters and (b) phase/amplitude differences of the designed balun BPF with about 50 Ω balanced impedance.

Table 1: Balanced impedance of the balun BPFs with open stub.

W_{UB}	W_B	W_1	L_1	L_2	L_3	Balanced impedance, Ω
2	2	0	0	0	0	250
2	1.75	2.5	5.5	12.25	11	100
2	1.5	2	14.5	8.25	9.5	50

was about 35 mm × 22.23 mm, as shown in Figure 6(a), and the photograph of the fabricated balun BPF is shown in Figure 6(b). Measurements were carried out using an Agilent N5071C network analyzer. Figures 7(a) and 7(b) show the full-wave simulated and measured results of the S-parameters and phase/amplitude differences for the circuit with balanced impedance of 100 Ohm, and that measured balanced impedance was about 50 Ohm at 2.6 GHz. Figures 8(a) and 8(b) show those for the circuit with balanced impedance of 50 Ohm, and that measured balanced impedance was about $(36 + j6)$ Ohm at 2.6 GHz.

The measured S_{ds21} values at the center frequencies of each passband in Figures 7(a) and 8(a) were 2.46 dB and 2.51 dB, respectively. The measured 3 dB band-edge frequencies of S_{ds21} values were observed at $f_{L,100\,\Omega} = 2.52$ GHz and $f_{H,100\,\Omega} = 2.7$ GHz for Figure 7(a) and were observed at $f_{L,50\,\Omega} = 2.53$ GHz and $f_{H,50\,\Omega} = 2.73$ GHz for Figure 8(a), respectively. The simulated and measured S_{cs21} values were smaller than 25 dB within operating bands of two balun BPFs. Those results demonstrate that our designed balun BPFs have good common-mode suppression at the differential output ports. Figures 7(b) and 8(b) also show that the amplitude difference between S_{21} and S_{31} is below 0.4 dB and the phase difference between S_{21} and S_{31} is within $180 \pm 7^\circ$ at operating

band. The proposed balun BPFs present a wide bandwidth, because they have two resonant frequencies within the passband. In this study, the designed balun BPF is based on a pair of half-wavelength OLRRs. Electrical coupling can be obtained if the open sides of the two coupled resonators are placed near each other. The balance impedance will improve the electrical performance of return loss, as shown in Figures 7(a) and 8(a), for that there is only one peak or two peaks that are observed. The little differences between the simulated and measured results in Figures 6 and 7 are mainly caused by the fabrication error (circuit etching), the SMA connector, and numerical error.

4. Conclusions

We presented a simple and effective method to design and fabricate a microstrip balun BPF with differential outputs. The dimensions for the proposed balun BPFs with balanced impedance of 100 Ohm and 50 Ohm were 35 mm × 23.98 mm and 35 mm × 22.23 mm, respectively. For the circuit with balanced impedance of 100 Ohm, that measured balanced impedance was about 50 Ohm at 2.6 GHz and for the circuit with balanced impedance of 50 Ohm, that measured balanced impedance was about $(36 + j6)$ Ohm at 2.6 GHz. The measured S_{ds21} values at the center frequencies for balanced impedance of 100 Ohm and 50 Ohm were 2.46 dB and 2.51 dB, respectively. The measured 3 dB band-edge frequencies of S_{ds21} values were observed at $f_{L,100\,\Omega} = 2.52$ GHz and $f_{H,100\,\Omega} = 2.7$ GHz and were observed at $f_{L,50\,\Omega} = 2.53$ GHz and $f_{H,50\,\Omega} = 2.73$ GHz for balanced impedance of 100 Ohm and 50 Ohm, respectively. By adjusting the physical dimensions of the OLRRs, the center frequencies of the balun BPF could be tuned over a wide range and the balanced impedance was tuned easily by open stub and W_B. In this study, not only the fabricated balun BPFs possessed good band-pass characteristics, but also the two balun BPFs had the good performance.

Conflict of Interests

The authors declare that there is no conflict of interests regarding the publication of this paper.

Acknowledgments

The authors acknowledge financial supports of MOST 103-2221-E-230-013 and MOST 103-2221-E-390-026.

References

[1] L. K. Yeung and K.-L. Wu, "A dual-band coupled-line balun filter," *IEEE Transactions on Microwave Theory and Techniques*, vol. 55, no. 11, pp. 2406–2411, 2007.

[2] L.-H. Zhou, H. Tang, J.-X. Chen, and Z.-H. Bao, "Tunable filtering balun with enhanced stopband rejection," *Electronics Letters*, vol. 48, no. 14, pp. 845–847, 2012.

[3] G.-S. Huang and C. H. Chen, "Dual-band balun bandpass filter with hybrid structure," *IEEE Microwave and Wireless Components Letters*, vol. 21, no. 7, pp. 356–358, 2011.

[4] C.-Y. Liou and S.-G. Mao, "Triple-band marchand balun filter using coupled-line admmittance inverter technique," *IEEE Transactions on Microwave Theory and Techniques*, vol. 61, no. 11, pp. 3846–3852, 2013.

[5] J. Shi and Q. Xue, "Dual-band and wide-stopband single-band balanced bandpass filters with high selectivity and common-mode suppression," *IEEE Transactions on Microwave Theory and Techniques*, vol. 58, no. 8, pp. 2204–2212, 2010.

[6] E.-Y. Jung and H.-Y. Hwang, "A balun-BPF using a dual mode ring resonator," *IEEE Microwave and Wireless Components Letters*, vol. 17, no. 9, pp. 652–654, 2007.

[7] D. M. Pozar, *Microwave Engineering*, Wiley, New York, NY, USA, 2nd edition, 1998.

[8] Q. Xue, J. Shi, and J.-X. Chen, "Unbalanced-to-balanced and balanced-to-unbalanced diplexer with high selectivity and common-mode suppression," *IEEE Transactions on Microwave Theory and Techniques*, vol. 59, no. 11, pp. 2848–2855, 2011.

[9] W. R. Eisenstadt, R. Stengel, and B. M. Thompson, *Microwave Differential Circuit Design Using Mixed-Mode S-Parameters*, Artech House, Boston, Mass, USA, 2006.